Topological study of charge densities of impurity doped small Li clusters

Tunna Baruah and D. G. Kanhere
Department of Physics, University of Pune, Pune-411007, India

Rajendra R. Zope
Commissariat à l'Energie Atomique Grenoble, Département de Recherche Fondamentale sur la Matière Condensée, 17 rue des Martyrs, F-38054 Grenoble, Cedex 9, France

(Received 24 October 2000; published 16 May 2001)

A topological analysis of charge densities in Li_nMg and Li_nBe clusters for $n=1-6$ is presented. Li_nBe clusters show a stronger bonding of the Li atoms with Be, as compared to Li_nMg clusters. The topology of the density shows that direct bonds between Li and impurity atoms have some closed-shell nature. Li-Li bonds are observed for clusters $n\leqslant 4$ in Li_nMg series, while for $n\geqslant 5$, the Li atoms form bonds only with the impurity atom. The bonds in some of the clusters seem to be strained. In contrast to Mg, the direct bonding of Be atom with the host indicates the tendency of Be to become trapped.

DOI: 10.1103/PhysRevA.63.063202 PACS number(s): 36.40.Wa

I. INTRODUCTION

The field of cluster physics has gained immense importance over the last decade due to the potential of designing nanomaterials with predecided characteristics [1,2]. Clusters often show properties which are much different from the bulk. The evolution of the properties with size as the cluster grows has been the focus of attention. Apart from homoatomic clusters, impurity-doped or mixed clusters have also been studied extensively in recent years. The impurity doping changes the nature of the bonds in the host clusters [3], and hence their properties. It was observed that doping with an impurity may even result in new magic numbers. Therefore, it is important to investigate how an impurity affects the bonding between the host atoms.

In this paper we present a systematic study of the topology of charge density in small Li clusters doped with divalent impurity atoms — Mg and Be. The ground-state geometries and electronic structure properties of these systems were studied by several groups [4,5]. Bulk LiMg, with different concentrations of the components, has been extensively studied due to its technological importance [6]. It is a lightweight material widely used in the aircraft industry. However, such an extensive study of this material in cluster form has not been performed so far. Earlier studies of ground-state geometries and the stability of Mg- and Be-doped Li clusters showed that these two isoelectronic impurities affect the host systems differently, resulting in different geometries for the same host cluster. Conventional analyses of such clusters were carried out on the basis of energetics, the energy gap between the highest occupied molecular orbital and lowest unoccupied molecular orbital, and charge-density contours.

It has been established that the topology of the charge density and its Laplacian can yield clear insight into the bonding mechanism in molecules [7]. First proposed by Bader, this method has been widely used in quantum-chemical studies of molecules, and to some limited extent in clusters. The method gives information about the charge density in the valence region where bonding takes place. The present work investigates the bonding characteristics of small Li_n clusters for $n=1-6$, doped with Mg and Be on the basis of charge-density topology. Such a topological study of pure Li clusters was performed by several groups [8–10]. These studies showed that in Li_2 clusters the density accumulates between the nuclei, and this piled up density can be termed as a topological pseudoatom which acts as glue binding the Li atoms. The presence of such maxima was also noted in the case of other metals — in Na clusters, metallic Be, etc. [9,11]. It was speculated whether the presence of such pseudoatoms signifies a trend toward forming a metallic bond. Although such maxima are known to be sensitive to the choice of basis set and electron-electron correlation [10], in the case of Li it was found that such pseudoatoms persist even with the inclusion of electron-electron correlation. Recently Pendás *et al.* [12] showed that the formation of maxima can be explained by promolecular densities. The present work analyzes the bonding of impurity-doped Li_n clusters on the basis of critical points of charge density and their properties.

In Sec. II, we give a brief description of a few concepts involved in the ''atoms in molecules'' studies which are utilized in the present work. Results and a discussion are presented in Sec. III.

II. THEORY AND COMPUTATIONAL DETAILS

A topological analysis of the charge density involves identifying the critical points where the gradient of density $\vec{\nabla}\rho(\vec{r})$ vanishes [7]. The critical points can be of different types depending on the eigenvalues ($\lambda_i, i=1$ and 3) of the Hessian at these points. The points of interest (n,m) are those with $n=3$ and $m=-3$, -1, 1, and 3, where n is the rank of the Hessian (number of nonzero eigenvalues) and m is the index defined as the sum of the signs of the eigenvalues. The point $(3,-3)$ identifies a maximum in the charge density which occurs naturally at nuclear sites. The maxima which occur at positions other than the nuclear sites are termed nonnuclear maxima. Bond critical points (BCP's) refer to the points $(3,-1)$ which occur between two bonding

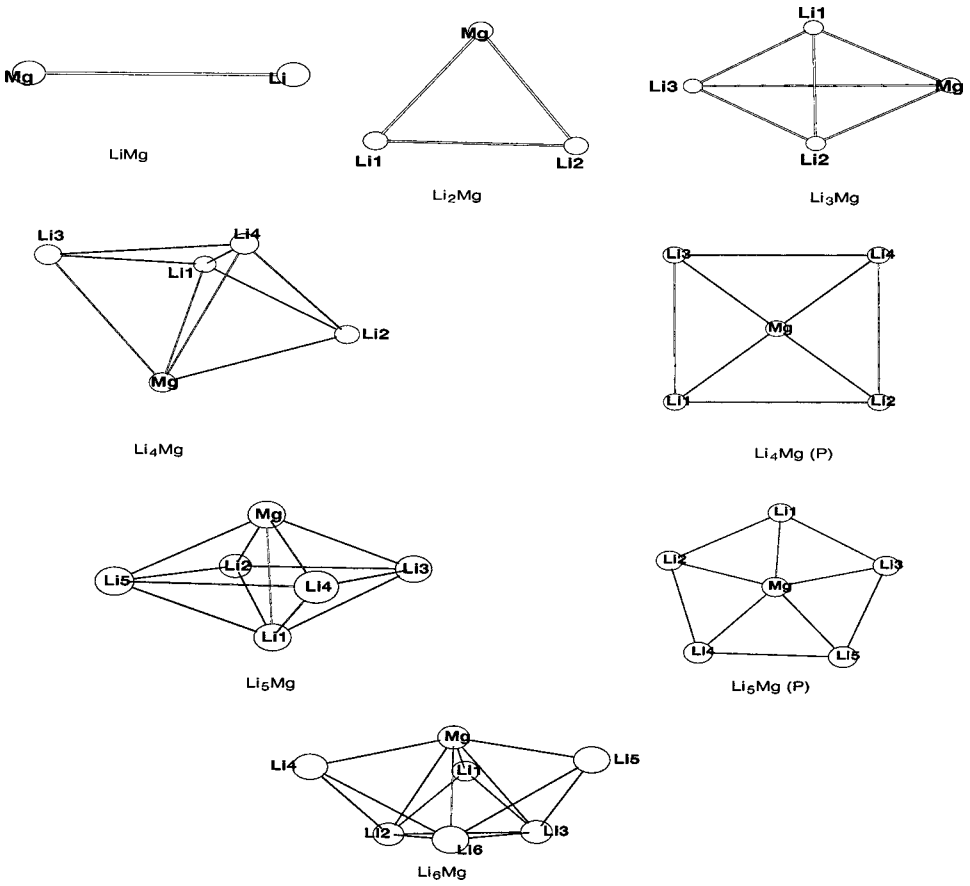

FIG. 1. Ground-state and low-lying geometries of Li_nMg clusters. (*P*) denotes the planar structures.

nuclei. The ring critical point (RCP), denoted by (3,1), occurs at the center of the ring formed by BCP's. At the cage critical point all the eigenvalues are positive, and these points occur between two rings. In a molecule or cluster, the number of critical points must satisfy the Poincaré-Hopf relationship

$$\sum_p (-1)^m = 1,$$

where the sum is over the critical points p and m is its index.

A useful method for the visualization of the topology of

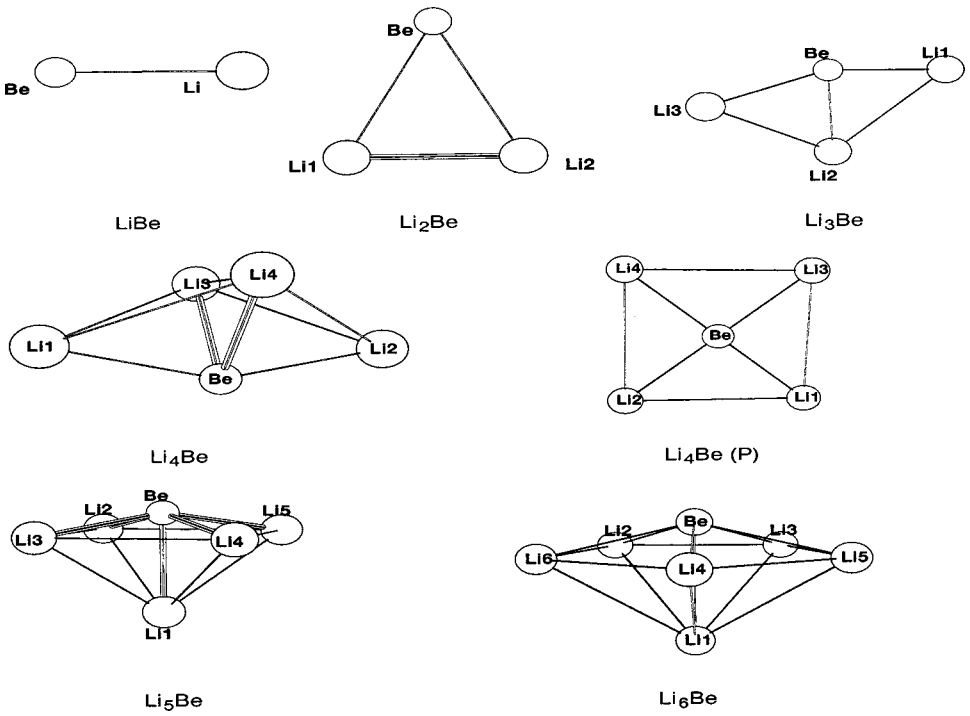

FIG. 2. Ground-state and low-lying geometries of Li_nBe clusters. (*P*) denotes the planar structures.

TABLE I. Table showing the values of ρ, $\nabla^2\rho$, and $|\lambda_1|/\lambda_3$, and the ellipticity of density at the BCP's. All values are in a.u.

System	ρ_b	$\nabla^2\rho_b$	$\lvert\lambda_1\rvert/\lambda_3$	Ellipticity
LiMg	0.0091	0.0076	0.2564	0.0001
LiBe	0.0155	0.0327	0.2054	0.0001

the density is via its gradient vector maps. Each nucleus is surrounded by a set of gradient vectors which terminate on the attractor or the maxima at the nuclei positions. This set of gradient vectors constitutes what is known as an atomic basin. Each nuclei has a corresponding basin, and each basin is separated by an interatomic surface. This is a zero-flux surface, since no trajectories of gradient vectors cross this surface. The maxima together, with their basin, define an ''atom'' in molecules. Between two bonding nuclei, the density is at a maximum along a curve linking them. This curve is called a bond path (BP). The existence of a bond path between two nuclei is a criteria to identify a bond between them, i.e., two nuclei form a bond only when there is a bond path connecting them. The BCP occurs where a bond path intersects the interatomic surface separating the two atoms.

The value of density at bond critical point (ρ_b) yields the bond order [13]. Thus a larger value of ρ_b indicates a stronger bond. Another important quantity in identifying the type of bond is the value of the Laplacian of density ($\nabla^2\rho_b$) at the BCP. It can be shown that, locally,

$$\boldsymbol{\nabla}^2\rho(\vec{r}) = 2G(\vec{r}) + V(\vec{r}),$$

where $G(\vec{r})$ is the kinetic-energy density and $V(\vec{r})$ is the potential energy [14]. A negative value of the Laplacian signifies a dominant contribution of the potential energy, and hence identifies the interaction to be of a shared nature. A positive value, on the other hand, shows the interaction to be of the opposite kind—typical of ionic, van der Waal, or hydrogen bonds [15]. The eigenvalues λ_i of the Hessian show the local curvatures of the density, and they are ordered as $\lambda_1 < \lambda_2 < \lambda_3$. The value of $|\lambda_1|/\lambda_3 < 1$ is indicative of closed-shell interactions.

The present calculations use the ground-state geometries of the Li_nMg and Li_nBe clusters obtained by the *ab initio* molecular-dynamics method, together with the simulated annealing technique, as the initial geometries [4]. These structures were further relaxed using the GAUSSIAN98 package [16] within the density-functional realm. An all-electron 6-31G* basis set was used, and the calculations were carried out within the three-parameter hybrid generalized gradient approximation (GGA) due to Becke *et al.* (B3LYP) [17]. This approach is based on the adiabatic connection method, and is currently the most powerful density-functional scheme that provides results close to those obtained by most refined post Hartree-Fock methods [18]. The use of the GGA permits us to incorporate the nonlocal effects of the gradient correction to the exchange-correlation potential into the electronic density, and hence its topology. The resulting electronic density was analyzed using the MORPHY [19] package.

TABLE II. Table showing the values of ρ, $\nabla^2\rho$, and $|\lambda_1|/\lambda_3$, and the ellipticity at the BCP's in Li_2A (A=Mg and Be). All values are in a.u.

System	BCP	ρ_b	$\nabla^2\rho_b$	$\lvert\lambda_1\rvert/\lambda_3$	Ellipticity
Li_2	Li-NNM	0.0113	0.0061	0.2788	0.0
Li_2Mg	Li-NNM	0.0129	0.0029	0.3993	0.1193
	Mg-NNM	0.0074	−0.0003	0.6300	0.3658
Li_2Be	Li-NNM	0.0130	0.0036	0.4238	0.5345
	Be-NNM	0.0129	−0.0054	1.5944	0.2215

III. RESULTS AND DISCUSSION

The lowest-energy state geometries of the Li_nMg and Li_nBe clusters are presented in Figs. 1 and 2 for the sake of completeness. The planar low-lying structures of a few selected clusters which are studied are also shown. The energetics of the ground-state and low-lying geometries of these clusters, obtained by *ab initio* molecular dynamics employing a simulated annealing technique, are described in Ref. [4]. A comparison of the geometries with those reported in Ref. [4] shows that the order of the isomers of Li_2Mg, Li_2Be, Li_3Mg, Li_4Be, and Li_6Be are reversed within the GGA. In the figures the Li atoms are numbered to facilitate a direct relation between the atoms shown in figures and described in the tables. The various properties of density at the BCP's of clusters of both series from $n=1$ to 6 are presented in Tables I–VI, respectively. In the tables, bonds in a given cluster with similar characteristics are grouped together. The gradient vectors and contours of density in Li_nMg, for $n=1-5$, are shown in Figs. 3, 5, 7, 9, and 11, respectively. The contours of the Laplacian of the density of LiBe and the gradient vector paths in Li_3Be and Li_4Be are presented in Figs. 4, 8, and 10, respectively. In the gradient vector maps the bond paths and interatomic surfaces are shown by dark lines. The BCP's and RCP's are shown as dark squares and triangles, respectively. For nonplanar clusters, the plots are shown in selected planes.

The critical points of density and their properties in LiMg and LiBe are summarized in Table I. Since both systems show a similar density gradient vector map, we present only the one for LiMg in Fig. 3. The figure shows one bond critical point on the interatomic surface separating the two atoms. From Table I, it is clear that the LiBe bond is stronger than the LiMg bond. In both systems, the values of $|\lambda_1|/\lambda_3$

TABLE III. Table showing the values of ρ, $\nabla^2\rho$, and $|\lambda_1|/\lambda_3$, and the ellipticity of the density at the bond critical points in Li_3 and Li_3Be. All values are in a.u.

System	BCP (A-B)	ρ_b	$\nabla^2\rho_b$	$\lvert\lambda_1\rvert/\lambda_3$	Ellipticity
Li_3Mg	$Li_{1,2}$-NNM	0.0111	0.0067	0.3375	0.4994
	Li_3-NNM	0.0130	0.0032	0.4540	0.8308
	Mg-NNM	0.0089	−0.0007	0.8385	1.3006
	Mg-$Li_{1,2}$	0.0094	0.0136	0.2424	0.9056
Li_3Be	$Li_{1,3}$-Be	0.0186	0.0372	0.2003	0.0363
	Li_2-Be	0.0124	0.0358	0.1528	1.9538

TABLE IV. Table showing the values of ρ, $\nabla^2\rho$, and $|\lambda_1|/\lambda_3$, and the ellipticity of the density at the bond critical points in Li_4Mg and Li_4Be. The same for planar structures denoted by (*P*) are also presented. All values are in a.u.

System	BCP (*A*-*B*)	ρ_b	$\nabla^2\rho_b$	$\lvert\lambda_1\rvert/\lambda_3$	Ellipticity
Li_4Mg	NNM_1-NNM_2	0.0115	−0.0023	1.3934	1.0087
	Li_1-$NNM_{1,2}$	0.0117	0.0082	0.2653	0.8952
	Li_2-NNM_1	0.0127	0.0053	0.3383	0.6754
	Li_3-NNM_2	0.0127	0.0053	0.3383	0.6732
	Li_4-$NNM_{1,2}$	0.0117	0.0082	0.2639	0.8643
	Mg-$NNM_{1,2}$	0.0129	−0.0041	2.0424	0.4448
$Li_4Mg(P)$	Li_{1-4}-Mg	0.0157	0.0182	0.2780	0.7804
Li_4Be	$Li_{1,2}$-Be	0.0177	0.0335	0.2211	0.3459
	Li_3-Be	0.0145	0.0398	0.1307	1.1841
	Li_4-Be	0.0121	0.0111	0.2014	5.0320
$Li_4Be(P)$	$Li_{1,2}$-Be	0.0227	0.0501	0.2175	0.3503
	Li_3-Be	0.0193	0.0597	0.1328	0.9954
	Li_4-Be	0.0188	0.0433	0.1915	1.3915

and $\nabla^2\rho_b$ show the bond to have a closed-shell nature. The integration of the charge density in each atomic basin in LiMg yields electronic charges of 2.6908 for Li and 12.3092 for Mg. Similarly, in LiBe, the Li basin has an electronic charge 2.4892, while Be has 4.5098. The eletronegativity of the Be atom is 1.5, while that of Mg is 1.2. This fact is reflected in the values of the electronic charge in the Be and the Mg basins. The closed-shell nature of the interaction is clearly visible from the contours of the Laplacian of density in LiBe (Fig. 4), with the contours bunching around each atom.

The next clusters in the series, Li_2Mg and Li_2Be, are triangular in their ground states. These structures are similar to the low-lying structures found in the earlier work [4] with the local density approximation (LDA). Both clusters show a non-nuclear maximum (NNM) of density between the two Li atoms (Fig. 5). The bond paths show the three nuclei to be connected to these NNM's rather than to each other. Li_2Be also shows a similar map, with the maxima slightly pulled toward the Be atom (not presented). The appearance of the NNM's in these clusters can be understood from the bonding in Li_2, where the charge density shows a maximum between the two atoms and the atoms are connected via this maximum [8]. For reference, we present the gradient vector map of Li_2 in Fig. 6, which shows two interatomic surfaces separating the Li atoms from the maximum at the middle. The NNM, along with its basin, constitutes a pseudoatom. However, it may be mentioned here that the appearance of the pseudoatom in Li is attributed to the rather large bond length of Li_2; decreasing the separation between the Li atoms results in the disappearance of the pseudoatom [8]. The bond critical points of Li_2, Li_2Mg, and Li_2Be, along with their properties, are presented in Table II. The binding of the impurity atom with the pseudoatom can be interpreted as a weak binding with the host cluster. From Table II it can be seen that Be has a higher bond order and a lower bond length than Mg. This can again be attributed to the higher electronegativity of the Be atom.

The structures of the lowest-energy state of Li_3Mg and Li_3Be are planar, with tetragonal shapes (Figs. 7 and 8). The structure of Li_3Mg, reported in Ref. [4], is slightly elongated in the present calculations. In Li_3, an NNM occurs at the center of the triangle formed by the three Li atoms. The pure Li clusters also show a similar kind of bonding, where the Li atoms favor a triangular formation with one maxima at the center. The Mg atom in this cluster is bound to the nearest two Li atoms, as well as to the pseudoatom. The characteristics of the BCP's are presented in Table III. The Mg-Li direct bonds are weak, and have a closed-shell nature. The high ellipticities of these bonds indicate a directional charge buildup in the plane perpendicular to the BP. On the other

TABLE V. Table showing the values of ρ, $\nabla^2\rho$, and $|\lambda_1|/\lambda_3$, and the ellipticity of the density at the bond critical points in Li_5Mg and Li_5Be. The superscript denotes the number of bond paths occurring between the same pair of atoms. All values are in a.u.

System	BCP (*A*-*B*)	ρ_b	$\nabla^2\rho_b$	$\lvert\lambda_1\rvert/\lambda_3$	Ellipticity
Li_5Mg	Li_1-$Mg^{(2)}$	0.0106	0.0062	0.2376	0.4006
	Li_{2-5}-Mg	0.0116	0.0067	0.2921	5.4786
$Li_5Mg(P)$	Li_{1-5}-Mg	0.0155	0.0185	0.2504	1.1170
Li_5Be	Li_1-Be	0.0156	0.0462	0.0757	1.6452
	$Li_{2,5}$-Be	0.0190	0.0430	0.1862	0.2865

TABLE VI. Table showing the values of ρ, $\nabla^2\rho$, and $|\lambda_1|/\lambda_3$, and the ellipticity of the density at the bond critical points in Li_6Mg and Li_6Be. The superscript denotes the number of bond paths occurring between the same pair of atoms. All values are in a.u.

System	BCP (*A*-*B*)	ρ_b	$\nabla^2\rho_b$	$\lvert\lambda_1\rvert/\lambda_3$	Ellipticity
Li_6Mg	$Li_{1,4,5}$-$Mg^{(2)}$	0.0109	0.0105	0.1614	0.2398
	$Li_{2,3,6}$-Mg	0.0136	0.0105	0.2626	0.9633
Li_6Be	Li_1-Be	0.0124	0.0305	0.0590	0.0045
	Li_{2-6}-Be	0.0171	0.0345	0.1812	0.4135

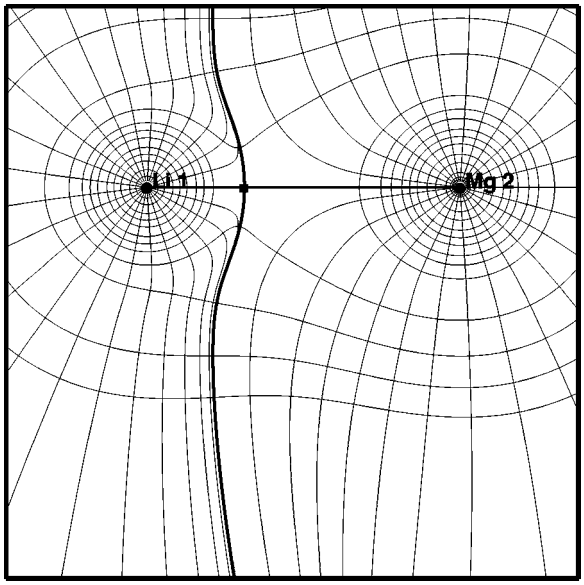

FIG. 3. Gradient vector paths in LiMg.

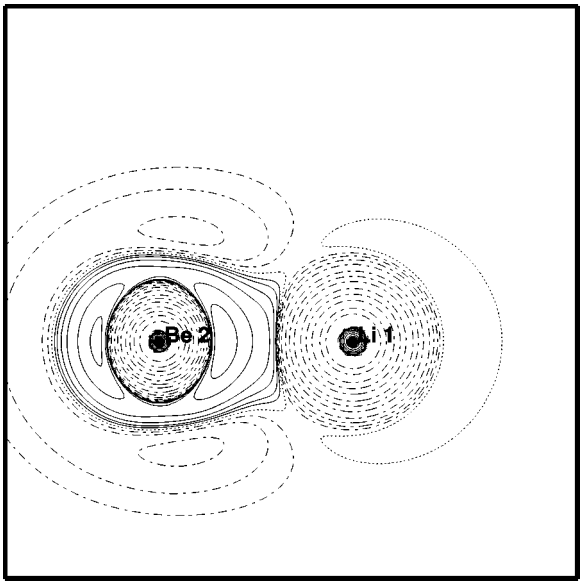

FIG. 4. Contours of Laplacian of density in LiBe. The negative-valued contours are shown as solid lines, and the positive-valued ones as dashed lines.

hand, Li_3Be shows a significantly different bonding. The NNM's seen in Li_3 are absent here, and all three Li atoms form direct bonds with Be (Fig. 8). There is no bond formed between the Li atoms — either direct or via NNM. The value of the Laplacian of density at all the three bond critical points are positive, indicating some ionic character of the Li-Be bonds. We expect that the direct bond formation of Be would favor a trapping of the Be in the host cluster as the cluster size grows. Indeed, this is borne out by earlier studies [4] of these clusters, where Mg occupies a surface position in the cluster while Be is trapped.

The trend seen for $n=3$ continues in clusters with $n=4$. These clusters form three-dimensional structures in the ground state, while planar structures are higher in energy. The order of isomers of Li_4Be seen within the LDA [4] is reversed within the GGA. The properties of the BCP's for both systems are presented in Table IV. The trend of Li atoms to form triangles is also seen here, with the four Li atoms forming a quintet roof structure in both Li_4Mg and Li_4Be. Both the triangles in Li_4Mg have one NNM at the center. It may be mentioned here that pure Li_4 favors a planar tetragonal structure, with two NNM's at the centers of the two triangles [8]. The gradient vector map shown in Fig. 9 and the value of $\nabla^2\rho_b$ (Table IV) show that the NNM's form weak shared bond between them. This feature is also seen in the pure Li_4 cluster [8]. Two RCP's occur on both sides of the BCP between NNM at distances 0.57 a.u. This feature suggests an unstable structure, since it takes a small amount of energy for them to coalesce, and then the structure may collapse. The Mg atom is connected to both the non-nuclear maxima. One more ring critical point occurs in this structure between the Mg atom and the NNM (Fig. 9), causing the outward bend of the bond paths. Although the Mg-NNM bond shows a closed-shell character in all Li_nMg clusters studied so far, we do not attach much significance to a bond between a real atom and a pseudoatom.

In Li_4Be, the NNM's are absent, and the formation of Li-Li bonds is also missing. The Li-Be distance is significantly smaller in this cluster, implying that the Be atom is more tightly bound to the host atoms than the Mg atom. In this case all the Li atoms are bound to the Be atom. As seen in other Li_nBe clusters, the LiBe bond has some ionic character, as is evident from the values of the Laplacian at the BCP's (Table IV). One of the Li-Be bonds shows a high value of ellipticity (~ 5), which indicates that this bond is somewhat strained (Fig. 10). To check the stabilities of these clusters, we have also repeated calculations for the planar structures for both Li_4Mg and Li_4Be. The planar structure of Li_4Mg was reported to be a low-lying structure in the *ab*

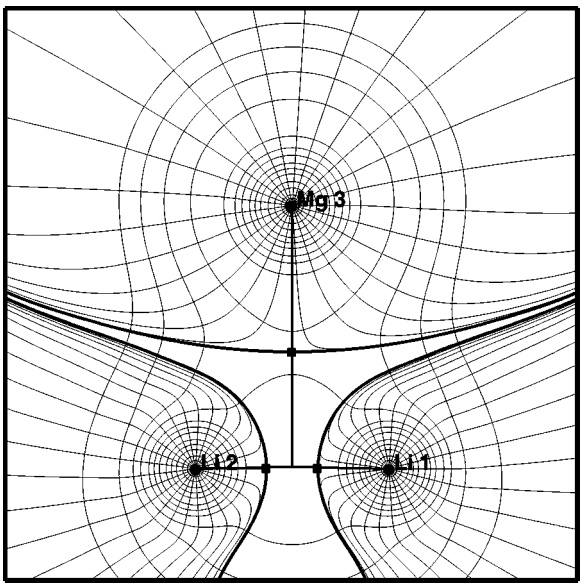

FIG. 5. Gradient vector paths in Li_2Mg.

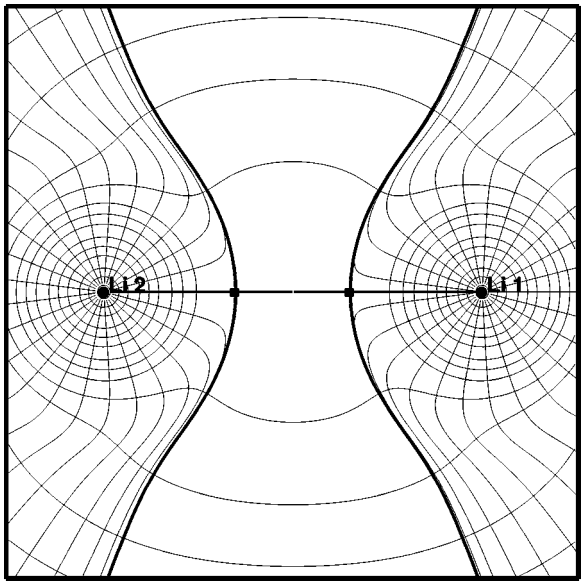

FIG. 6. Gradient vector paths in Li_2.

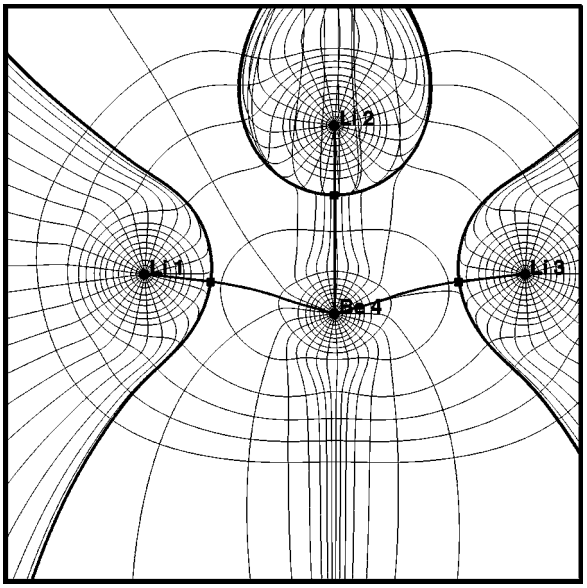

FIG. 8. Gradient vector paths in Li_3Be.

initio molecular-dynamics calculation with a simulated annealing technique, while the lowest-energy structure of Li_4Be was found to be the planar one [4]. Since these structures are significantly different from the present lowest-energy structures, we decided to contrast the bondings between them. The characteristics of the BCP's of the planar structures are also included in Table IV. It is apparent that planar structures are more stable with direct bonds of higher order in both systems. Another point to be noted is that both impurities form bonds with some ionic character. The NNM are missing in the planar structures. However, the ellipticity values show that bonds are also somewhat strained in these structures.

Clusters with $n=5$ in both series show some similarity in the lowest-energy state structures of the Li cage. In both systems the Li atoms form a pyramid, while the impurity atom is capped to the base. The Be atom lies nearer to this base than Mg. The Li atoms bind only to the Be atom similar to the Li_4Be cluster. The bonds with the nearest Li atoms are stronger than those with an apical one (Table V). The bonds with the four base atoms show similar characteristics. No NNM is formed in this cluster either. The Laplacian at all five BCP's is positive, indicating closed-shell-type bonds. The bond ellipticity is also small, suggesting a stable structure. On the other hand, Li_5Mg shows a significantly different type of topology than the other Li_nMg clusters. The nonnuclear maxima are not observed, and all the Li atoms are directly connected only to the Mg atom. However, the BCP's between Mg and base Li atoms do show a high value of

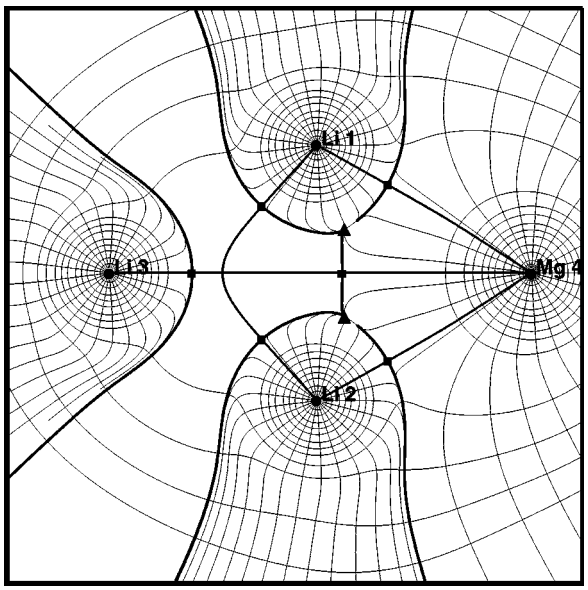

FIG. 7. Gradient vector paths in Li_3Mg.

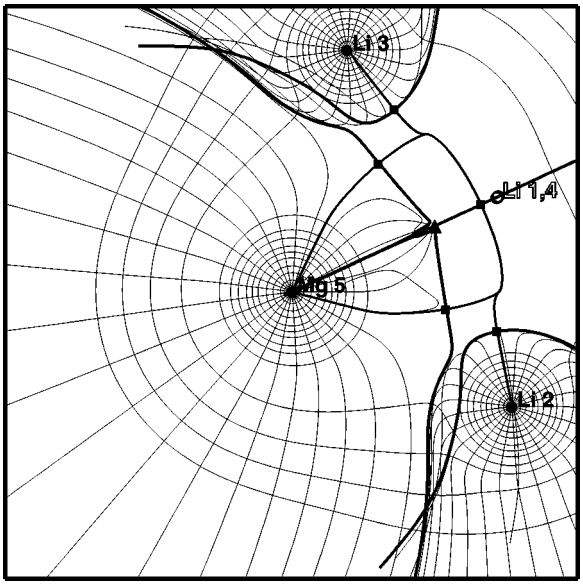

FIG. 9. Gradient vector paths in Li_4Mg.

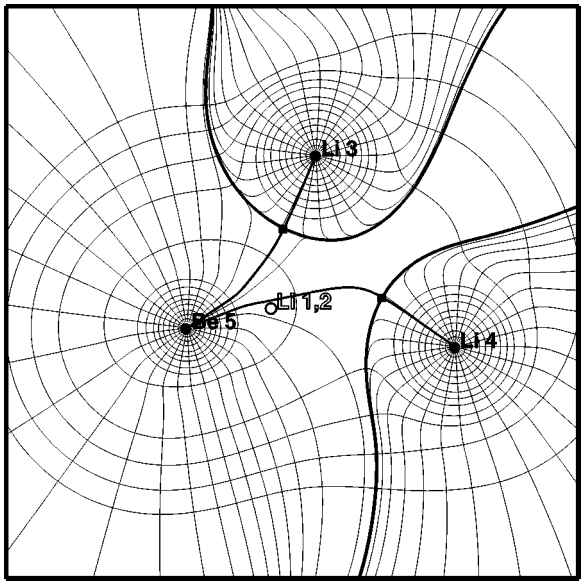

FIG. 10. Gradient vector paths in Li_4Be.

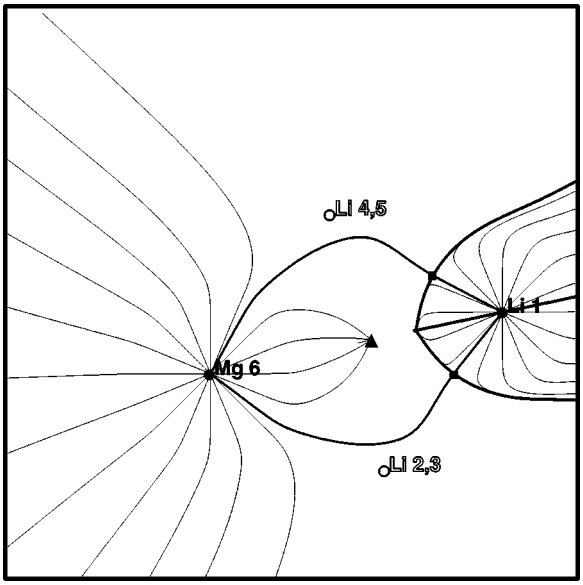

FIG. 11. Gradient vector paths in Li_5Mg in the plane of Mg and the apical Li atom.

ellipticity ~ 5, suggesting a large strain on the bond (Table V). The two long curvaceous bond paths connecting the apical Li atom with the Mg atom are shown in Fig. 11. The BP's curve away from the ring critical point at the center of the cluster. The Laplacians of density at BCP's suggest some ionic character to all the Li-Mg bonds. We contrast the bonding of the ground-state cluster with a planar pentagonal structure with higher energy. This planar structure was found to be a low-lying structure in an earlier calculation with a simulated annealing technique. In this case, the Mg sits in the middle, and all the Li atoms are connected to it. The bond orders are higher than in the other structure, the bonds showing some ionic character. All the bonds have almost similar characteristics. However, the ellipticities of the bonds indicate that they are strained.

The ground-state structures of Li_6Mg and Li_6Be show more stable bonding than the others. It may be mentioned here that a reversal of order of the isomers is observed in Li_6Be with the GGA. The properties of the BCP's in these two structures are presented in Table VI. While all the Li atoms are connected only to the impurity atom in both cases, the bonds in Li_6Mg connecting Mg with the nearest Li atoms show more curvature. Two bond paths connect each of these atoms to Mg. These bond paths deviate around a ring critical point. The bonds in this case can be classified into two groups, as presented in Table VI. The structural symmetry is also reflected in the two groups of bonds. The bonds in Li_6Be are stronger than those in Li_6Mg. Also in this case, the bonds with the atoms at the base of the pentagon are identical. The interaction is seen to be of closed-shell nature in both systems. NNM are absent in these clusters.

In conclusion, the bonding mechanism in small Li_nMg and Li_nBe are different, although the structures of these small clusters are somewhat similar. While both impurities are divalent, Be has a higher eletronegativity than Mg, and therefore the Li-Be bond has some ionic character. In Li_nMg, for $n \leqslant 4$, the Li atoms tend to form a triangular face, with one non-nuclear maximum at the center, and the Mg forms a weak bond with the cluster. The nature of binding in the host cluster is only slightly affected by the presence of Mg. While the Li atoms do form a bond with the NNM's, there is no direct Li-Li bond present. In case of Li_nBe, the NNM's shift toward the Be due to its high electronegativity. In the Li_nBe clusters, except for $n=2$, there is no Li-Li bond in either direct or via non-nuclear maxima. Interestingly, there is some similarity between Li_nMg and Li_nBe for $n=5$ and 6, in that both Mg and Be forms direct bonds with Li atoms, and the interaction is of closed-shell nature. There is no NNM present in these clusters. Another point to be noted is that direct bonds in both series show some ionic character.

It emerges from this analysis that the direct bonds seen between Li and Be are much stronger than the indirect ones via NNM observed in certain Li_nMg clusters. In larger clus-

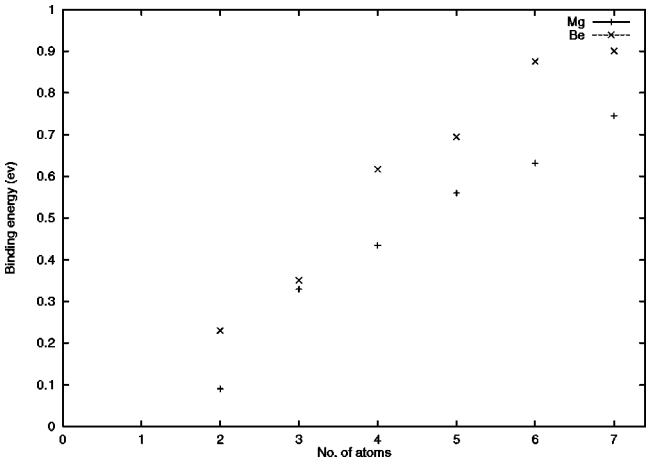

FIG. 12. Binding energies per atom of Li_nMg and Li_nBe clusters.

ters, for $n \geqslant 5$, the NNM's disappear, and the bonds in these systems are stronger. It was seen that Li_nBe clusters are structurally more stable than the same host doped with Mg. This fact is also borne out by the relatively higher binding energy per atom in Be-doped Li clusters than those doped with Mg (Fig. 12). Interestingly, for $n=2$, where the binding is similar for both Mg and Be, the binding energies are also comparable.

ACKNOWLEDGMENTS

T.B. is thankful to Dr. R. K. Pathak, Dr. S. A. Kulkarni for valuable discussions, and M. Deshpande for help. All of the authors gratefully acknowledge financial support from the Indo-French Center for Promotion of Advanced Research (New Delhi)/Center Franco-Indien Pour la Promotion de la Recherche Avancée.

[1] W. A. de Heer, Rev. Mod. Phys. **65**, 611 (1993).
[2] W. P. Halperin, Rev. Mod. Phys. **58**, 533 (1986).
[3] M. M. Kappes, P. Radi, M. Schar, and E. Schumacher, Chem. Phys. Lett. **119**, 11 (1985).
[4] M. D. Deshpande, A. J. Dhavale, R. R. Zope, S. Chacko, and D. G. Kanhere, Phys. Rev. A **62**, 063202 (2000).
[5] Rong-qi-Tang, Phys. Rev. B **43**, 9255 (1991); P. Fantucci, V. Banacic-Koutecky, and J. Koutecky, Z. Phys. D: At., Mol. Clusters **12**, 307 (1989); P. Fantucci, V. Bancic-Koutecky, W. Pewestorf, and J. Koutecky, J. Chem. Phys. **91**, 4229 (1989); W. Pewestorf, V. Bonacic-Koutecky, and J. Koutecky, *ibid.* **89**, 5794 (1988).
[6] G. Bruno, B. Ginatempo, E. S. Giuliano, and A. Stancanelli, Nuovo Cimento D **9**, 1495 (1987); S. Das and H. C. Fraser, in *Proceedings Light Weight Alloys for Aerospace Applications*, edited E. W. Lee, E. H. Chia, and N. J. Kim (TMS, Warrendale, PA, 1989); I. J. Polmear, *Light Alloys — Metallurgy of Light Metals* (Chapman and Hall, New York, 1989).
[7] R. F. W. Bader, *Atoms in Molecules: A Quantum Theory* (Oxford University Press, Oxford, 1990).
[8] C. Gatti, P. Fantucci, and G. Pachchioni, Theor. Chim. Acta **72**, 433 (1987).
[9] W. L. Cao, C. Gatti, P. J. MacDougall, and R. F. W. Bader, Chem. Phys. Lett. **141**, 380 (1987).
[10] K. Edgecombe, R. O. Esquival, V. H. Smith, Jr., and F. Muller-Plathe, J. Chem. Phys. **97**, 2593 (1992).
[11] B. B. Iversen, F. K. Larsen, M. Souhassou, and M. Takata, Acta Crystallogr., Sect. B: Struct. Sci. **51**, 580 (1995); D. Jayatilaka, Phys. Rev. Lett. **80**, 798 (1998); C. Mei, K. E. Edgecombe, V. H. Smith, Jr., and A. Heilingbrunner, Int. J. Quantum Chem. **48**, 287 (1992).
[12] A. Martín Pendás, M. A. Blanco, A. Costales, P. M. Sánchez, and V. Luaña, Phys. Rev. Lett. **83**, 1930 (1999).
[13] R. F. W. Bader, T. S. Slee, D. Cremer, and E. Kraka, J. Am. Chem. Soc. **105**, 5061 (1983).
[14] R. F. W. Bader, Chem. Rev. **91**, 893 (1991).
[15] R. F. W. Bader and H. Essén, J. Chem. Phys. **80**, 1943 (1984).
[16] GAUSSIAN98, M. J. Frisch *et al.*, Gaussian Inc., Pittsburgh, PA, 1998.
[17] A. D. Becke, Phys. Rev. A **38**, 3098 (1988); C. Lee, W. Yang, and R. G. Parr, Phys. Rev. B **37**, 785 (1988).
[18] V. Barone, J. Chem. Phys. **101**, 6834 (1994); V. Baker, J. Andzelm, M. Munir, and P. R. Taylor, Chem. Phys. Lett. **237**, 53 (1995); C. W. Bauschlicher, *ibid.* **246**, 40 (1995).
[19] P. L. A. Popelier, Comput. Phys. Commun. **93**, 212 (1996).